Wavelength conversion for single-photon polarization qubits through continuous-variable quantum teleportation

Xi-Wang Luo,[1] Chuanwei Zhang,[1,*] Irina Novikova,[2] Chen Qian,[3] and Shengwang Du[1,†]
[1]*Department of Physics, The University of Texas at Dallas, Richardson, Texas 75080, USA*
[2]*Department of Physics, William and Mary, Williamsburg, Virginia 23187, USA*
[3]*Department of Computer Science and Engineering, University California Santa Cruz, Santa Cruz, California 95064, USA*

(Received 7 October 2021; accepted 11 May 2022; published 31 May 2022)

A quantum internet connects remote quantum processors that need to interact and exchange quantum signals over a long distance through photonic channels. However, these quantum nodes operate at the wavelength ranges unsuitable for long-distance transmission. Therefore, quantum wavelength conversion to telecom bands is crucial for long-distance quantum networks based on optical fiber. Here, we propose wavelength conversion devices for single-photon polarization qubits using continuous-variable quantum teleportation that can efficiently convert qubits between near-infrared (780–795 nm suitable for interacting with atomic quantum nodes) and telecom wavelength (1300–1500 nm suitable for long-distance transmission). The teleportation uses entangled photon fields (i.e., nondegenerate two-mode squeezed state) that can be generated by four-wave mixing in a rubidium atomic gas using a diamond configuration of atomic transitions. The entangled fields can be emitted in two orthogonal polarizations with locked relative phase, making them especially suitable for interfacing with single-photon polarization qubits. Our work may pave the way for the realization of long-distance quantum networks.

DOI: 10.1103/PhysRevA.105.052444

I. INTRODUCTION

Quantum technologies have been intensively developed in recent years [1–3]. Long-distance quantum communication is crucial for unconditional security as well as connecting remote quantum processors through a quantum internet [4,5]. A quantum internet is expected to be more powerful than the simple sum of each quantum nodes, enabling a number of revolutionary applications such as quantum networks of clocks [6] and distributed quantum computing. The realization of a quantum internet relies on the long-distance communication between remote quantum processors through photonic channels [4,5]. However, single-photon qubits emitted from these quantum nodes (such as atomic ensembles [7] and trapped ions [8]), often in the visible or near-infrared (NIR) regions, are usually unsuitable for long-distance transmission. Moreover, interconnections between disparate quantum systems are impossible due to their mismatched emission wavelengths [2,4,5,9]. Quantum wavelength conversion (QWC) [10], which enables the spectral translation of a photon to a targeted wavelength without disturbing its quantum properties, is a solution to these issues.

QWC between NIR and telecom bands [11] is one of the most important wavelength conversions since telecom band photons remain the information carriers of choice for long-distance transmission based on optical fibers, while NIR photons not only interact with atomic quantum systems but also fall into the working band of many high-performance single-photon detectors [12] and quantum memories [13]. For long-distance communication between remote quantum nodes, one first uses the QWC device to convert the single-photon qubit emitted by quantum node *A* from NIR to telecom wavelength, then sends it to quantum node *B* through fiber transmission, and finally converts its wavelength back to the NIR band for interacting with the quantum processor (as illustrated in Fig. 1). QWC between NIR and telecom bands has been demonstrated for a wide range of quantum systems (e.g., trapped ions and rubidium gas) [14–21]. However, these QWC devices are usually directly realized through three- or four-wave nonlinear optical mixing, which face difficulties of noise photons and low conversion efficiency (30–70%) for the photonic interface.

In this paper, we propose wavelength conversion devices for single-photon polarization qubits using continuous-variable (CV) quantum teleportation [22–26]. Such hybridization of discrete variables (DVs) and CVs overcomes the probabilistic restriction of DV-only teleportation which relies on unambiguous two-qubit Bell-state measurement [27]. The entangled fields of the CV teleportation are nondegenerate two-mode squeezed vacuum (TMSV) states. By performing a joint homodyne measurement of a single photon and one of the entangled fields at the same NIR (telecom) wavelength, we can teleport single-photon qubit into the telecom (NIR) band by imprinting the measured joint quadratures into the other entangled field at the shifted wavelength. The use of a hybrid technique involving CV teleportation of a DV (i.e., polarization qubits) allows deterministic wavelength conversion of photonic qubits with ∼100% efficiency. In addition to teleportation, combining DVs and CVs in hybrid architectures may offer significant advantages in quantum computation and information processing [28–37].

*Chuanwei.Zhang@utdallas.edu
†dusw@utdallas.edu

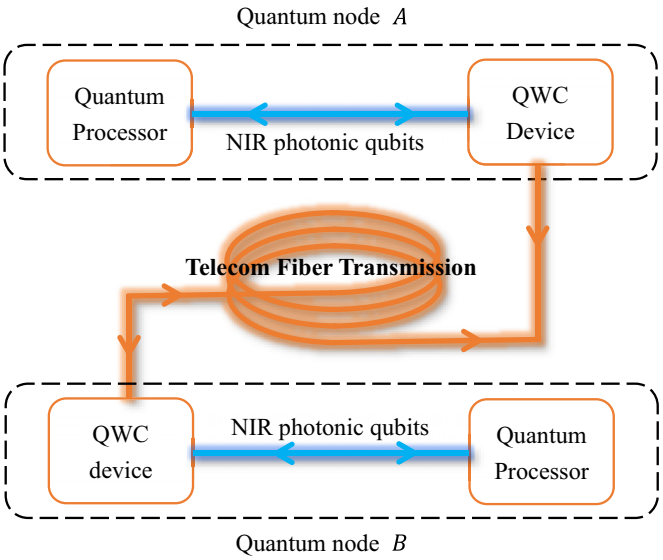

FIG. 1. Illustration of long-distance communication between remote quantum nodes.

Homodyne measurements [38] require using light of known polarization; therefore, two polarizations need to be teleported parallelly, and each polarization component of the qubit requires a TMSV entangled state for the teleportation. Additional phase locking between the two polarization teleporters (i.e., the two TMSV entangled states) is necessary to avoid any phase errors in the teleportation. Such phase locking is still challenging even for ordinary CV teleportation without wavelength conversion, where the degenerate TMSV entangled fields are generated by mixing two identical single-mode squeezed states at a 50:50 beam splitter.

To realized QWC, we need to use *nondegenerate* TMSV states which cannot be generated by mixing single-mode squeezed states. Here, we propose generating nondegenerate TMSV entangled fields using a four-wave mixing (FWM) process in a Rubidium atomic gas with a diamond configuration of atomic transitions [39–42]. In this process, the wavelength of one field matches the single photon emitted from the atomic quantum nodes, while the other falls into the telecom-band optical fields that are suitable for low-loss fiber transmission. Because of the symmetry, the TMSV states can be emitted in two orthogonal polarizations with fixed relative phase, making them especially suitable for interfacing with polarization single-photon qubits. Our approach provides an attractive alternative to nonlinear crystal-based wavelength conversions that typically have low efficiency and require tremendous technical care. Note that, although we only discuss QWC between NIR (780–795 nm) and telecom (1300–1500 nm) wavelengths in this paper, the CV teleportation-based wavelength conversion can be easily generalized to a wide range of frequencies if suitable two-color squeezed states can be generated using nonlinear optical mixing.

II. QWC THROUGH CV TELEPORTATION

Quantum teleportation [43] is a technique for transferring quantum information from a sender at one location to a receiver some distance away, by sending only classical information and using a shared entangled state as a resource. It has become one of the key elements of practical quantum information protocols. Originally, quantum teleportation was proposed for DV qubits, and significant progress has been made in demonstrating quantum teleportation of photonic qubits. However, most of these schemes share one fundamental restriction: they require unambiguous two-qubit Bell-state measurements which are always probabilistic (with a success probability of 50%) when linear optics is used [44].

The concept was later generalized to CV teleportation [22], which relies on the quadrature-entangled states (i.e., two-mode squeezed states) [45] and the measurements in the quadrature bases using linear optics and homodyne detection, leading to deterministic teleportation without postselection. Homodyne measurement corresponds to projection measurement of the field in the coherent state basis. Due to the correlated quadratures of the two entangled fields (modes A and B), a joint Homodyne measurement of a single photon and mode A of the entangled fields projects mode B of the entangled fields into a displaced single-photon state (intuitively, the state of mode B after projection can be understood as a certain combination of a single photon and a coherent state). Therefore, we can perform proper displacement of mode B to obtain a single-photon state. So far, CV teleportation has been demonstrated for unconditional teleportation of quantum states such as the nonclassical CV state and time-bin qubits with fixed polarization [27,46–50]. Since homodyne measurements require light of known polarization, one needs a pair of such entangled states with locked relative phase to parallelly teleport the two components of the polarization qubits.

We consider nondegenerate two-mode squeezed states generated by the following Hamiltonian:

$$H_{\rm sq} = \sum_{s=H,V} [i\xi_s \hat{a}^\dagger_{A,s}\hat{a}^\dagger_{B,s} + \text{H.c.}], \tag{1}$$

which leads to squeezing between modes A and B for both polarizations H and V. Here, $\hat{a}^\dagger_{A,B}$ are the photon creation operators of modes A and B, with corresponding frequencies $\omega_{A,B}$ falling in the NIR and telecom bands, respectively. The entangled state $|\text{ES}\rangle = \exp(-iH_{\rm sq}\tau)|\text{vac}\rangle$ is generated by evolving the vacuum under the Hamiltonian $H_{\rm sq}$ for a certain time period τ. We obtain a pair of TMSV states $|\text{ES}\,\rangle_\Omega = \prod_s \hat{S}_s(r_s)|\text{vac}\rangle$, with $\hat{S}_s(r) = \exp(r\hat{a}^\dagger_{A,s}\hat{a}^\dagger_{B,s} - \text{H.c.})$ as the two-mode squeezing operator [45,51] for polarization s and $r_s = \xi_s\tau$ as the squeezing factor. We assume $r_H = r_V = r$ are real; therefore, a pair of in-phase nondegenerate TMSV states are generated coherently.

In the photon number basis, the entangled fields can be written as [25]

$$\begin{aligned}|\text{ES}\rangle &= (1-q^2)\sum_{n,m} q^{n+m}|n;m\rangle_A|n;m\rangle_B \\ &= (1-q^2)\sum_{n,N} q^N|n;N-n\rangle_A|n;N-n\rangle_B,\end{aligned} \tag{2}$$

where $|n;N-n\rangle$ represents n photons in H polarization and $N-n$ photons in V polarization, and $q = \tanh(r)$. We want to teleport a single-photon polarization qubit

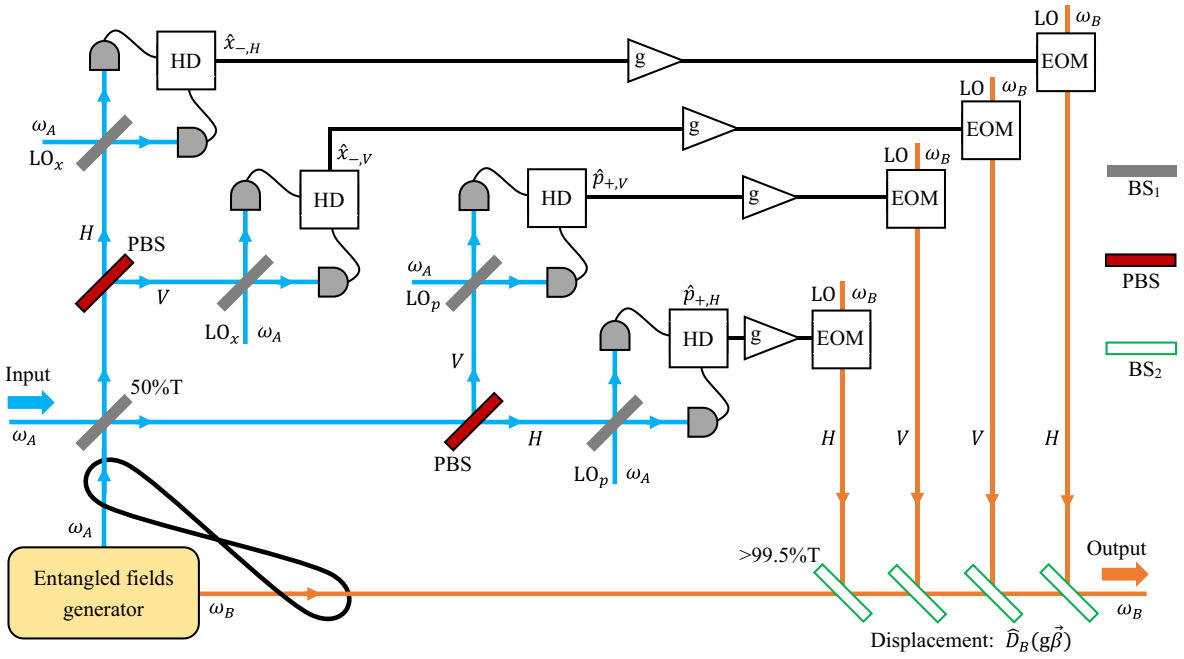

FIG. 2. Schematic illustration of the quantum wavelength conversion device based on continuous-variable (CV) quantum teleportation. BS_1 and BS_2 represent the beam splitters with 50% and >99.5% transmittance, respectively; PBS, HD, and EOM represent polarizing beam splitter, homodyne detector, and electro-optic modulator. LO_x and LO_p are local oscillators with frequency ω_A for Homodyne detection of x and p quadratures in mode A, respectively. LO is the local oscillator with frequency ω_B for the displacement operation of mode B. In experiments, these local oscillators are typically obtained in the same cell, and local oscillators with different frequencies are generated independently.

$|\psi\rangle_{\rm in} = c_1|1;0\rangle_{\rm in} + c_2|0;1\rangle_{\rm in}$ and convert its frequency from ω_A to ω_B.

The QWC device based on the CV teleportation process is schematically illustrated in Fig. 2. First, we combine the input mode $|\psi\rangle_{\rm in}$ with mode A at a 50:50 beam splitter and make the balanced homodyne detection of mode $\hat{a}_{\pm,s} = \frac{\hat{a}_{{\rm in},s} \pm \hat{a}_{A,s}}{\sqrt{2}}$, with $\hat{a}_{{\rm in},s}$ as the input field operator for polarization s. We use a local oscillator with frequency ω_A to measure $\hat{x}_{-,s} = (\hat{a}_{-,s} + \hat{a}^\dagger_{-,s})/\sqrt{2}$ and $\hat{p}_{+,s} = i(\hat{a}^\dagger_{+,s} - \hat{a}_{+,s})/\sqrt{2}$, which generate the control signal $\vec{\beta} = (\beta_H, \beta_V)$, where $\beta_s = \langle \hat{x}_{-,s} + i\hat{p}_{+,s}\rangle$, and $\langle\cdot\rangle$ corresponds to the detection projection. The homodyne measurement projects the state of input $|\psi\rangle_{\rm in}$ and A modes to the state:

$$|\vec{\beta}\rangle_{{\rm in},A} = \frac{1}{\pi}\sum_{n,m} \hat{D}_{\rm in}(\vec{\beta})|n;m\rangle_{\rm in}|n;m\rangle_A, \tag{3}$$

with displacement operator $\hat{D}_{\rm in}(\vec{\beta}) = \prod_s \exp(\beta_s \hat{a}^\dagger_{{\rm in},s} - \beta^*_s \hat{a}_{{\rm in},s})$. Then we perform the displacement $g\vec{\beta}$ on mode B using a local oscillator with frequency ω_B and accomplish the teleportation. Here, g is the gain factor, and the output state (unnormalized) in mode B becomes

$$|\psi\rangle_{\rm out} = {}_{{\rm in},A}\langle\vec{\beta}|\hat{D}_B(g\vec{\beta})|{\rm ES}\rangle|\psi\rangle_{\rm in} = \hat{T}_q(\vec{\beta})|\psi\rangle_{\rm in}, \tag{4}$$

where

$$\hat{T}_q(\vec{\beta}) = \frac{1-q^2}{\pi}\sum_{n,m} q^{n+m}\hat{D}_B(g\vec{\beta})|n;m\rangle_{B\,{\rm in}}\langle n;m|\hat{D}_{\rm in}(-\vec{\beta})$$

is the transfer operator. In the strong squeezing limit, we have $\hat{T}_q(\vec{\beta}) \propto \sum_{n,m}|n;m\rangle_{B\,{\rm in}}\langle n;m|$ for unit gain $g = 1$, and the normalized output state reads

$$|\psi\rangle_{\rm out} = c_1|1;0\rangle_B + c_2|0;1\rangle_B, \tag{5}$$

which is identical to the input state $|\psi\rangle_{\rm in}$, except that the frequency of the qubit is shifted from ω_A to ω_B. The teleportation process corresponds to one-photon teleportation in H (V) polarization and a vacuum teleportation in V (H) polarization. Similarly, we can convert the wavelength of the photonic qubit from ω_B to ω_A.

To generate the displacement on mode B, we can use electro-optical modulators (EOMs) to modulate the local oscillator (which has frequency ω_B) according to the homodyne detection signals and combine these phase-modulated beams with mode B at a beam splitter of >99.5% transmittance (as shown in Fig. 2). Moreover, we want to mention that the ideal two-mode squeezing requires infinite energy, and ideal CV entangled fields are physically unattainable; thus, the teleportation fidelity is generally limited by the squeezing factor. In this case, nonunit gain conditions are useful [27,52,53]. With proper choice of the gain factor $g = q = \tanh(r)$, no additional photons would be created in the output, and the teleported single-photon qubit remains undisturbed regardless of the squeezing level, with a success probability q^2 [27,52,53]. Therefore, the wavelength conversion efficiency (i.e., q^2) can be ~100% for sufficiently strong squeezing $\tanh(r) \to 1$.

We now discuss the dependence of the teleportation fidelity on the squeezing factor. First, we consider the teleportation with unit gain (i.e., $g = 1$) and assume the squeezing factors for both polarizations are the same. The fidelity is defined as the probability to successfully teleport a single-photon state in

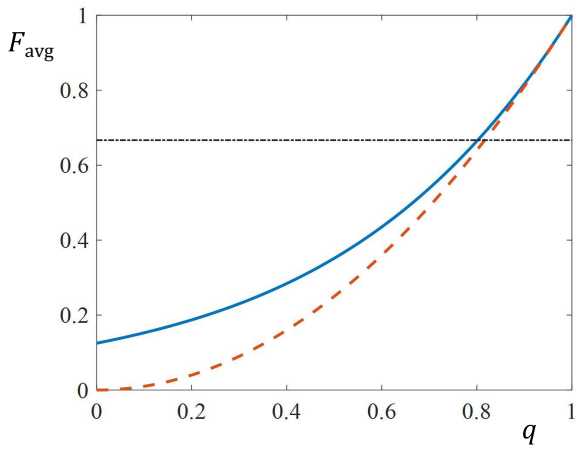

FIG. 3. Averaged fidelity F_{avg} of the teleportation as a function of squeezing factor q. The blue solid (red dashed) line corresponds to the unit (optimal) gain teleportation. The horizontal dash-dotted line corresponds to the classical fidelity limit $\frac{2}{3}$.

polarization H (V) and a vacuum state in polarization V (H). Without loss of generality, we can consider the teleportation of a single photon in H polarization with $c_1 = 1$ and $c_2 = 0$. The probability to obtain the measurement value β_H, β_V is $P_q(\vec{\beta}) = \langle\psi|\psi\rangle_{\text{out}} = \frac{1-q^2}{\pi}\exp[-(1-q^2)|\beta_H|^2][(1-q^2)^2|\beta_H|^2 + q^2]\frac{1-q^2}{\pi}\exp[-(1-q^2)|\beta_V|^2]$, and the probability to obtain the desired output state (i.e., a single-photon state in H polarization) is $P_q(\vec{\beta}, 1_H, 0_V) = |\langle 1_H; 0_V|\psi\rangle_{\text{out}}|^2 = P_q(\vec{\beta})\exp[-(1-q)^2|\beta_H|^2]\exp[-(1-q)^2|\beta_V|^2]$. This means that, for some measurement value $\vec{\beta}$, the probability to successfully teleport a single-photon state in polarization H (V) and a vacuum state in polarization V (H) is $\mathcal{F}_\beta = P_q(\vec{\beta}, 1_H, 0_V)/P_q(\vec{\beta}) = \exp[-(1-q)^2|\beta_H|^2]\exp[-(1-q)^2|\beta_V|^2]$. If we do not care what the value of $\vec{\beta}$ is, the averaged probability to obtain the desired output state reads $P_q(1_H, 0_V) = \int d\vec{\beta} P_q(\vec{\beta}, 1_H, 0_V) = \frac{1+q^2}{2}(\frac{1+q}{2})^2$, which gives the averaged fidelity $\mathcal{F}_{\text{avg}} = P_q(1_H, 0_V)$, as discussed in Ref. [25]. Here, $\mathcal{F}_{\text{avg}}$ would exceed the classical limit $\frac{2}{3}$ for $q \simeq 0.8$ (i.e., $r \simeq 1.1$), as shown in Fig. 3. The averaged probability to obtain zero-photon and multiphoton ($\geqslant 2$) output states is $P_{q,0} = \frac{1-q}{2}(\frac{1+q}{2})^2$ and $P_{q,\text{multi}} = 1 - \frac{5-4q+3q^2}{4}(\frac{1+q}{2})^2$. In addition, there is probability of a polarization flip while preserving the single-photon number with $P_{q,\text{flip}} = \frac{1-q^2}{2}(\frac{1+q}{2})^2$ (see Ref. [25] for more details). We see that a large $q \sim 1$ is required to obtain high fidelity and avoid creating additional photons.

On the other hand, one can use the optimal gain teleportation $g = q$ to avoid creating additional photons [27,52]. The output state now reads $|\psi\rangle_{\text{out}} = \frac{1-q^2}{\pi}\exp[-(1-q^2)\frac{(|\beta_H|^2+|\beta_V|^2)}{2}][(1-q^2)\beta_H^*|0_H; 0_V\rangle + q|1_H; 0_V\rangle]$, and we have considered the input state $|1_H; 0_V\rangle$ with $c_1 = 1$. For a general input state, the output state reads $|\psi\rangle_{\text{out}} \sim (c_1\beta_H^* + c_2\beta_V^*)(1-q^2)|0_H; 0_V\rangle + q|\psi\rangle_{\text{in}}$. The optimal gain teleportation will not introduce additional photons to the signal. It is easy to show that $\mathcal{F}_\beta = \frac{q^2}{q^2+(1-q^2)|\beta_H|^2}$ and $\mathcal{F}_{\text{avg}} = q^2$ (see Fig. 3). We want to mention that the fidelity becomes 100% if we postselect the state with photons in the signal channel, with the success probability q^2. In this sense, the efficiency of the wavelength converter is q^2 with 100% fidelity. Therefore, we can have high fidelity even for low squeezing factors, though the conversion efficiency q^2 would be low.

III. ENTANGLED FIELDS FROM FWM

The key element of our scheme is to generate a pair of nondegenerate TMSV states, where the wavelength of one mode in the TMSV state matches photons emitted from the quantum nodes, and the other mode falls into the telecom band. In this section, we show how to generate such nondegenerate two-mode squeezing through FWM.

As we discussed previously, homodyne measurements require using light of known polarization; therefore, two polarizations need to be teleported in parallel, and each polarization component of the qubit requires a TMSV entangled state. The relative phase between the two TMSV states should be locked. Suppose there is a random and unknown relative phase between the two polarizing TMSV states (i.e., we replace $\hat{a}_{A,V}$ and $\hat{a}_{B,V}$ by $\exp(-i\phi_A)\hat{a}_{A,V}$ and $\exp(-i\phi_B)\hat{a}_{B,V}$ in Eq. 1), then the entangled state becomes

$$|\text{ES}(\phi)\rangle = (1-q^2)\sum_{n,m} q^{n+m}e^{im\phi}|n; m\rangle_A|n; m\rangle_B,$$

with $\phi = \phi_A + \phi_B$ a random and unknown phase. The final output state becomes

$$|\psi(\phi)\rangle_{\text{out}} = c_1|1; 0\rangle_B + c_2e^{i\phi}|0; 1\rangle_B, \tag{6}$$

with a phase error. Therefore, even the ordinary CV teleportation (without wavelength conversion) of a single-photon polarization qubit is still challenging and has not been demonstrated experimentally since a TMSV state generated by mixing two identical single-mode squeezed states usually has an unknown relatively phase with respect to other TMSV states generated in the same way.

Here, we consider the FWM in a rubidium atomic gas [39–42,54–56], with a diamond configuration of atomic transitions, as shown in Fig. 4(a). The ground state $5S_{1/2}$ is coupled to the excited state $4D_{3/2}$ through a two-photon process, with intermediate states $5P_{1/2}$ or $5P_{3/2}$. The setup is schematically shown in Fig. 4(b). An ensemble of ^{87}Rb

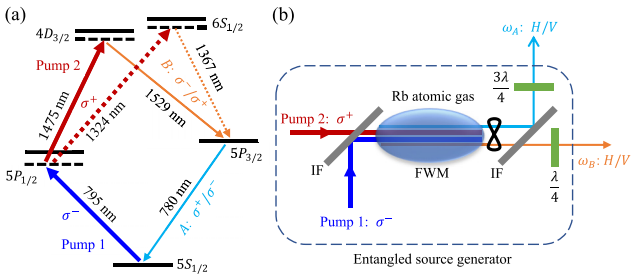

FIG. 4. Illustration of the four-wave mixing (FWM) process to generate two-mode squeezing. (a) Level scheme for the FWM in ^{87}Rb. (b) Schematic of the proposed entangled field generator. IF represents the interference filter. The $\frac{3\lambda}{4}$ and $\frac{\lambda}{4}$ wave plates are used to convert $\sigma^\pm$ to H/V polarizations.

atoms is trapped with a magneto-optical trap. All atoms are initialized to ground state $5S_{1/2}$. In the FWM process, two pump lasers (with NIR wavelength $\lambda_1 = 795$ nm and telecom $\lambda_2 = 1475$ nm, respectively) are used to excite atoms to state $4D_{3/2}$ with intermediate state $5P_{1/2}$. Then state $4D_{3/2}$ decays back to $5S_{1/2}$ through parametric down conversion with intermediate state $5P_{3/2}$, followed by the generation of photon pairs (with telecom wavelength $\lambda_B = 1529$ nm and NIR wavelength $\lambda_A = 780$ nm, respectively). The Hamiltonian of the FWM process can be written as

$$H_{\mathrm{FWM}} = \chi^{(3)}\, \hat{a}_1 \hat{a}_2 \hat{a}_A^\dagger \hat{a}_B^\dagger + \mathrm{H.c.}, \tag{7}$$

where $\chi^{(3)}$ is the third-order nonlinear coefficient, and a_j is the annihilation operator for optical field λ_j. We can replace the field operator $\hat{a}_{1,2}$ of the pump lasers by the coherent amplitudes $\hat{\alpha}_{1,2}$, then $H_{\mathrm{FWM}} \to i\xi \hat{a}_A^\dagger \hat{a}_B^\dagger + \mathrm{H.c.}$, with $\xi = -i\chi^{(3)}\, \hat{\alpha}_1 \hat{\alpha}_2$ to be real for proper gauge choice. Energy conservation requires that the generated photon pairs in modes A and B have frequencies ω_A and ω_B, respectively, where $\omega_j = \frac{2\pi c}{\lambda_j}$ satisfies $\omega_A + \omega_B = \omega_1 + \omega_2$, and c is the speed of light.

Now we examine the polarizations of the two-mode squeezing fields generated by FWM. We consider that the four fields are in a copropagating geometry inside the atomic cloud, which satisfies the phase matching, as shown in Fig. 4(b). With the quantization axis along the beam propagation direction of all modes, we drive transitions with $\Delta m_F = \pm 1$ using two pump beams that are orthogonally circularly polarized. In the coherent parametric down-conversion process, the final quantum state of the atoms remains the same as the initial state. Furthermore, rotational symmetry of the atomic cloud along the beam-propagation direction implies angular momentum conservation. The angular momentum selection rules limit the polarizations of the generated photon pairs, and the Hamiltonian becomes

$$H_{\mathrm{FWM}} = i\xi(\hat{a}_{A,\sigma^+}^\dagger \hat{a}_{B,\sigma^-}^\dagger + s\hat{a}_{A,\sigma^-}^\dagger \hat{a}_{B,\sigma^+}^\dagger + \mathrm{H.c.}), \tag{8}$$

where $\sigma^\pm$ denote the left and right circular polarizations, respectively, and s is determined by the Clebsh-Gordan coefficients [41]. The pair generation process is coherent, with $\hat{a}_{A,\sigma_+}^\dagger \hat{a}_{B,\sigma_-}^\dagger$ and $\hat{a}_{A,\sigma_-}^\dagger \hat{a}_{B,\sigma_+}^\dagger$ indistinguishable and phase locked by the Clebsh-Gordan coefficients. That is $s = \frac{C^{F_m,1,F_e}_{m_F+1,-1,m_F} C^{F_g,1,F_m}_{m_F,1,m_F+1}}{C^{F_m,1,F_e}_{m_F-1,+1,m_F} C^{F_g,1,F_m}_{m_F,-1,m_F-1}}$, where F_g, F_e, and F_m are the total angular momentum of the participating ground state $5S_{1/2}$, excited state $4D_{3/2}$, and the intermediate state $5P_{1/2}$ or $5P_{3/2}$. If we choose the initial hyperfine ground state $|F_g, m_F = 0\rangle$, we have $s = 1$ for all F_g, F_e, and F_m. The problem for choosing $m_F = 0$ as the ground state is that atoms may be pumped to $m_F = -2$ in the FWM process due to the strong pumping laser, which can be overcome by using large detuned pumpings. It is worth mentioning that, for room temperature atoms, the Doppler shift is comparable or larger than the hyperfine splitting of the levels $5P_{3/2}$ and $4D_{3/2}$, which means that different F_e and F_m hyperfine states would participate in the process (even through the pump detunings are larger than the Doppler shift). Fortunately, we have $s = 1$ for all these hyperfine levels with $m_F = 0$.

Alternatively, we can use $|5S_{1/2}, F = 1, m_F = -1\rangle$ as the ground state and couple it to $|5P_{1/2}, F = 2, m_F = -2\rangle$ and then to $|5D_{3/2}, F = 3, m_F = -1\rangle$ through pumping lasers, followed by two-photon generation through $|5P_{3/2}, F = 2, m_F = -2\rangle$ or $|5P_{3/2}, F = 2, m_F = 0\rangle$. This FWM process also leads to $s = 1$. However, the problem is that the pumpings should be near resonance to avoid unwanted couplings with other hyperfine states (e.g., $|5D_{3/2}, F = 2, m_F = -1\rangle$). As a result, cold atoms must be used since room temperature atoms have a Doppler shift comparable or larger than the hyperfine splitting of the levels $5P_{3/2}$ and $4D_{3/2}$, which means that different F_e and F_m hyperfine states would participate in the process. In addition, pair generation may have multiple decay paths through different hyperfine levels of $5P_{3/2}$, and we need to use additional filters to select one decay path (i.e., $5P_{3/2}, F = 2$).

Finally, with proper local operations on the entangled fields $\hat{a}_{A,\sigma^\pm} \to \hat{a}_{A,HV}$ and $\hat{a}_{B,\sigma^\mp} \to \hat{a}_{B,HV}$, H_{FWM} reduces to H_{sq} in Eq. (1), and the FWM process generates two-mode squeezing for both polarizations with locked and known relative phase, which makes them especially suitable for teleporting single-photon polarization qubits. We can also use $\lambda_1 = 780$ nm and $\lambda_2 = 1529$ nm for the pump beams with $5P_{3/2}$ as the corresponding intermediate state, then obtain the two-mode squeezing with wavelengths $\lambda_A = 795$ nm and $\lambda_B = 1475$ nm. Moreover, we can choose a different atomic level such as $6S_{1/2}$ to be the high excited state [see Fig. 4(a)], which allows us to generate telecom fields with wavelengths 1324 and 1367 nm.

Experimentally, the squeezing factor is determined by the third-order nonlinear coefficient $\chi^{(3)}$, pumping laser intensities, and propagation time in the atomic gas. Here, $\chi^{(3)}$ and propagation time can be increased by using higher atomic density and longer atomic cell. To achieve averaged fidelity (efficiency) of $\frac{2}{3}$ for unit (optimal) gain teleportation, $q \simeq 0.8$ ($r \simeq 1.15$) is required. Improving the fidelity (efficiency) to 90% requires $q \simeq 0.95$ ($r \simeq 1.8$). We expect that the squeezing at this level can be achieved in realistic experiments with proper choices of the detunings and pumping intensities. Experiments [15,16] operating in the regime of FWM frequency conversion with Hamiltonian $H_{\mathrm{FWM}} = \xi' \hat{a}_2 \hat{a}_A^\dagger + \mathrm{H.c.}$ have achieved $\xi'\tau \simeq 0.8$ (since the FWM conversion efficiency is >50%) even though the excited and intermediate states are all far detuned (the detunings range from 10 to 40 MHz). For our FWM squeezing scheme, one of the intermediate states is in resonance with effective detuning, given by its level broadening which is about a few megahertz; therefore, ξ in the squeezing Hamiltonian $H_{\mathrm{FWM}} = \xi \hat{a}_B \hat{a}_A^\dagger + \mathrm{H.c.}$ can be several times larger than ξ' in the FWM frequency conversion scheme [15,16], leading to a squeezing parameter $r = \xi\tau > 2$. The corresponding CV teleportation-based conversion efficiency would be $q^2 > 0.93$. Moreover, similar FWM was explored for collimated blue light generation [57,58], in which strong two-photon emission has been observed under the range of experimental conditions, which also provides optimism for our proposal.

IV. FINITE QUBIT BANDWIDTH

We have assumed a single-frequency photonic qubit in the discussion above, while in practice the

photonic qubit always has a finite frequency bandwidth. In the Heisenberg picture, the balanced homodyne detection corresponds to projection measurement $\beta_s(t) = \langle \exp(i\omega_A t)\hat{a}_{\text{in},s}(t) - \exp(-i\omega_A t)\hat{a}^\dagger_{A,s}(t)\rangle$. After performing the displacement on mode B, the output fields are

$$\hat{a}_{\text{out},s}(t) = \hat{a}_{B,s}(t) + \exp(-i\omega_- t)\hat{a}_{\text{in},s}(t) - \exp(-i\omega_+ t)\hat{a}^\dagger_{A,s}(t), \tag{9}$$

with $\omega_\pm = \omega_B \pm \omega_A$. In the frequency domain, we have

$$\hat{a}_{\text{out},s}(\omega_B + \Omega) = \hat{a}_{\text{in},s}(\omega_A + \Omega) + \hat{a}_{B,s}(\omega_B + \Omega) - \hat{a}^\dagger_{A,s}(\omega_A - \Omega). \tag{10}$$

This means that we need two-mode squeezing between frequency component $\omega_A - \Omega$ in mode A and the frequency component $\omega_B + \Omega$ in mode B to convert a single-frequency qubit from $\omega_A + \Omega$ to $\omega_B + \Omega$.

Meanwhile, we can consider the finite squeezing bandwidth of the FWM process, and the Hamiltonian reads

$$H_{\text{FWM}} = i\xi \sum_{s,\Omega} [\hat{a}^\dagger_{A,s}(\omega_A - \Omega)\hat{a}^\dagger_{B,s}(\omega_B + \Omega) + \text{H.c.}], \tag{11}$$

due to energy conservation, with Ω taking values within the squeezing bandwidth. The Hamiltonian in Eq. (11) leads to exactly the desired squeezing. In the Heisenberg picture, the TMSV state satisfies $[\hat{a}_{B,s}(\omega_B + \Omega) - \hat{a}^\dagger_{A,s}(\omega_A - \Omega)]_{\text{TMSV}} = e^{-r}[\hat{a}_{B,s}(\omega_B + \Omega) - \hat{a}^\dagger_{A,s}(\omega_A - \Omega)]_{\text{vac}}$. In the strong squeezing limit, the output field in Eq. (10) becomes the same as the input field $\hat{a}_{\text{out},s}(\omega_B + \Omega) = \hat{a}_{\text{in},s}(\omega_A + \Omega)$, except the frequency is shifted by $\omega_B - \omega_A$. Therefore, our proposal works if the frequency bandwidth of the squeezing is sufficiently wide to cover the qubit bandwidth.

Our proposal works when the frequency bandwidth of the squeezing is comparable or greater than the frequency bandwidth of the qubit. Let us first consider the optimal gain teleportation. We can write the input/output state in the frequency domain as $|\psi\rangle_{\text{in}} = \int d\Omega A_{\text{in}}(\Omega)|\psi(\omega_A + \Omega)\rangle_{\text{in}}$ and $|\psi\rangle_{\text{out}} = \int d\Omega A_{\text{out}}(\Omega)|\psi(\omega_B + \Omega)\rangle_{\text{out}}$ with $\int d\Omega |A_{\text{in/out}}(\Omega)|^2 = 1$, and the output state reads $|\psi\rangle_{\text{out}} \sim q|\psi\rangle_{\text{in}}$. Successful teleportation leads to the output state as $|\psi\rangle_{\text{out}} \sim q|\psi\rangle_{\text{in}}$ with wavelength conversion, that is $A_{\text{out}}(\Omega) \sim q(\Omega)A_{\text{in}}(\Omega)$. The successful probability (i.e., averaged fidelity without postselection) is $\mathcal{F}_{\text{avg}} = \int d\Omega |q(\Omega)A_{\text{in}}(\Omega)|^2$. In the case that $q(\Omega)$ has a much wider frequency bandwidth than $A_{\text{in}}(\Omega)$ (e.g., with ratio 10:1), we roughly have $\mathcal{F}_{\text{avg}} = q^2(0)$ and $A_{\text{out}}(\Omega) \sim q(0)A_{\text{in}}(\Omega)$ [i.e., the output state satisfies $A_{\text{out}}(\Omega) \simeq A_{\text{in}}(\Omega)$ with little distortion in temporal profile compared with the input state]. Even if $q(\Omega)$ has a comparable frequency bandwidth as $A_{\text{in}}(\Omega)$, we have $\mathcal{F}_{\text{avg}} \simeq 0.7q^2(0)$ [we assume both $A_{\text{in}}(\Omega)$ and $q(\Omega)$ have a Gaussian profile]. In addition, the temporal profile of the output state is distorted through $A_{\text{out}}(\Omega) \sim q(\Omega)A_{\text{in}}(\Omega)$. Fortunately, this does not affect the information encoded in the polarization space. That is, once an output photon is detected with reduced probability $0.7q^2(0)$, the corresponding fidelity (after postselection) is still 100%. The effect of finite frequency bandwidth of the squeezing is similar for the unit gain teleportation, which would lead to temporal distortion and reduce the fidelity.

In experiments, the Doppler shift would broaden the frequency bandwidth of the squeezing. For cold atoms, the Doppler shift can be neglected, while for room temperature atoms, the Doppler shift is ∼200–300 MHz. We want to emphasize that, in the presence of a Doppler shift, the frequencies of the squeezed two modes are still given by $\omega_A + \Omega$ and $\omega_B - \Omega$. To avoid resonant pumpings and reduce the incoherent emission, we can use pump detunings larger than the Doppler shift so that most atoms remain in the initial ground state. In addition, polarization encoding would not be affected by the Doppler effect during the teleportation since the squeezing factors for two polarizations can still be the same and their relative phase is still locked. Moreover, the coherent two-photon emissions are exponentially amplified along the phase-matching direction which are employed as the entangled resource, while incoherent emissions with directions have negligible contributions along the phase-matching direction. Due to the broadened frequency bandwidth of the squeezing, the Doppler effects may degrade the squeezing and so the teleportation, which can be overcome by increasing atom numbers.

V. DISCUSSION AND CONCLUSIONS

We have shown how to realize the wavelength conversion for single-photon polarization qubits through CV teleportation and to generalize the nondegenerate two-mode squeezed entangled fields using FWM. For long-distance communication between remote quantum nodes, we can use the procedure as illustrated in Fig. 1. Alternatively, we can first send the telecom mode of the entangled fields from node A to B, then teleport the photonic qubit from node A to B with wavelength conversion, and finally convert the qubit back to the NIR wavelength at node B. For the later approach, additional photon loss may be introduced to the entangled fields during the transmission, which will reduce the teleportation fidelity [59].

In summary, we proposed a QWC device for single-photon polarization qubits using CV quantum teleportation. We considered a FWM process in rubidium atomic gas with a diamond configuration of atomic transitions to generate the entangled fields, which corresponds to a pair of in-phase nondegenerate TMSV states. One of the entangled fields has a wavelength of 780–795 nm, and the other has a wavelength of 1300–1500 nm, allowing efficiently wavelength conversion of single-photon qubits between NIR (suitable for interacting with atomic quantum nodes) and telecom wavelength (suitable for long-distance transmission). Moreover, it is possible to generate the wavelength conversion scheme to a wide range of frequencies if the corresponding two-color squeezed states can be generated by suitable nonlinear optical mixing. Our work provides an attractive alternative to a nonlinear crystal-based wavelength conversion that still has difficulty with noise photons and conversion efficiency.

ACKNOWLEDGMENTS

C.Z., I.N., C.Q., and S.D. acknowledge support from the U.S. Department of Energy (Award No. DE-SC0022069). X.-W.L. acknowledges support from the Air Force Office of Scientific Research (No. FA9550-20-1-0220) and the Army Research Office (No. W911NF-17-1-0128).

[1] Y. Alexeev, D. Bacon, K. R. Brown, R. Calderbank, L. D. Carr, F. T. Chong, B. DeMarco, D. Englund, E. Farhi, B. Fefferman *et al.*, Development of quantum interconnects (QuICs) for next-generation information technologies, PRX Quantum **2**, 017001 (2021).

[2] D. Awschalom, K. K. Berggren, H. Bernien, S. Bhave, L. D. Carr, P. Davids, S. E. Economou, D. Englund, A. Faraon, M. Fejer *et al.*, Development of quantum interconnects (QuICs) for next-generation information technologies, PRX Quantum **2**, 017002 (2021).

[3] E. Altman, K. R. Brown, G. Carleo, L. D. Carr, E. Demler, C. Chin, B. DeMarco, S. E. Economou, M. A. Eriksson, K.-M. C. Fu *et al.*, Quantum simulators: architectures and opportunities, PRX Quantum **2**, 017003 (2021).

[4] H. J. Kimble, The quantum internet, Nature (London) **453**, 1023 (2008).

[5] S. Wehner, D. Elkouss, and R. Hanson, Quantum internet: a vision for the road ahead, Science **362**, eaam9288 (2018).

[6] P. Kómár, E. M. Kessler, M. Bishof, L. Jiang, A. S. Sørensen, J. Ye, and M. D. Lukin, A quantum network of clocks, Nature Phys. **10**, 582 (2014).

[7] L.-M. Duan, M. D. Lukin, J. I. Cirac, and P. Zoller, Long-distance quantum communication with atomic ensembles and linear optics, Nature (London) **414**, 413 (2001).

[8] L.-M. Duan and C. Monroe, Colloquium: Quantum networks with trapped ions, Rev. Mod. Phys. **82**, 1209 (2010).

[9] M. Wallquist, K. Hammerer, P. Rabl, M. Lukin, and P. Zoller, Hybrid quantum devices and quantum engineering, Phys. Scr. **T137**, 014001 (2009).

[10] P. Kumar, Quantum frequency conversion, Opt. Lett. **15**, 1476 (1990).

[11] S. Tanzilli, W. Tittel, M. Halder, O. Alibart, P. Baldi, N. Gisin, and H. Zbinden, A photonic quantum information interface, Nature (London) **437**, 116 (2005).

[12] R. H. Hadfield, Single-photon detectors for optical quantum information applications, Nature Photon **3**, 696 (2009).

[13] N. Sangouard, C. Simon, H. de Riedmatten, and N. Gisin, Quantum repeaters based on atomic ensembles and linear optics, Rev. Mod. Phys. **83**, 33 (2011).

[14] R. Ikuta, Y. Kusaka, T. Kitano, H. Kato, T. Yamamoto, M. Koashi, and N. Imoto, Wide-band quantum interface for visible-to-telecommunication wavelength conversion, Nat. Commun. **2**, 537 (2011).

[15] A. Radnaev, Y. O. Dudin, R. Zhao, H. H. Jen, S. Jenkins, A. Kuzmich, and T. A. B. Kennedy, A quantum memory with telecom-wavelength conversion, Nat. Phys. **6**, 894 (2010).

[16] Y. O. Dudin, A. G. Radnaev, R. Zhao, J. Z. Blumoff, T. A. B. Kennedy, and A. Kuzmich, Entanglement of Light-Shift Compensated Atomic Spin Waves with Telecom Light, Phys. Rev. Lett. **105**, 260502 (2010).

[17] T. Walker, K. Miyanishi, R. Ikuta, H. Takahashi, S. V. Kashanian, Y. Tsujimoto, K. Hayasaka, T. Yamamoto, N. Imoto, and M. Keller, Long-Distance Single Photon Transmission from a Trapped Ion via Quantum Frequency Conversion, Phys. Rev. Lett. **120**, 203601 (2018).

[18] M. Bock, P. Eich, S. Kucera, M. Kreis, A. Lenhard, C. Becher, and J. Eschner, High-fidelity entanglement between a trapped ion and a telecom photon via quantum frequency conversion, Nat. Commun. **9**, 1998 (2018).

[19] Y. Yu, F. Ma, X.-Y. Luo, B. Jing, P.-F. Sun, R.-Z. Fang, C.-W. Yang, H. Liu, M.-Y. Zheng, X.-P. Xie *et al.*, Entanglement of two quantum memories via fibres over dozens of kilometres, Nature (London) **578**, 240 (2020).

[20] N. Maring, P. Farrera, K. Kutluer, M. Mazzera, G. Heinze, and H. de Riedmatten, Photonic quantum state transfer between a cold atomic gas and a crystal, Nature (London) **551**, 485 (2017).

[21] R. Ikuta, T. Kobayashi, T. Kawakami, S. Miki, M. Yabuno, T. Yamashita, H. Terai, M. Koashi, T. Mukai, T. Yamamoto *et al.*, Polarization insensitive frequency conversion for an atom-photon entanglement distribution via a telecom network, Nat. Commun. **9**, 1997 (2018).

[22] L. Vaidman, Teleportation of quantum states, Phys. Rev. A **49**, 1473 (1994).

[23] S. L. Braunstein and H. J. Kimble, Teleportation of Continuous Quantum Variables, Phys. Rev. Lett. **80**, 869 (1998).

[24] A. Furusawa, J. L. Sørensen, S. L. Braunstein, C. A. Fuchs, H. J. Kimble, and E. S. Polzik, Unconditional quantum teleportation, Science **282**, 706 (1998).

[25] T. Ide, H. F. Hofmann, T. Kobayashi, and A. Furusawa, Continuous-variable teleportation of single-photon states, Phys. Rev. A **65**, 012313 (2001).

[26] S. Bose and H. Jeong, Quantum teleportation of hybrid qubits and single-photon qubits using Gaussian resources, Phys. Rev. A **105**, 032434 (2022).

[27] S. Takeda, T. Mizuta, M. Fuwa, P. van Loock, and A. Furusawa, Deterministic quantum teleportation of photonic quantum bits by a hybrid technique, Nature (London) **500**, 315 (2013).

[28] P. van Loock, T. D. Ladd, K. Sanaka, F. Yamaguchi, K. Nemoto, W. J. Munro, and Y. Yamamoto, Hybrid Quantum Repeater Using Bright Coherent Light, Phys. Rev. Lett. **96**, 240501 (2006).

[29] J. B. Brask, I. Rigas, E. S. Polzik, U. L. Andersen, and A. S. Sørensen, Hybrid Long-Distance Entanglement Distribution Protocol, Phys. Rev. Lett. **105**, 160501 (2010).

[30] P. van Loock, W. J. Munro, K. Nemoto, T. P. Spiller, T. D. Ladd, S. L. Braunstein, and G. J. Milburn, Hybrid quantum computation in quantum optics, Phys. Rev. A **78**, 022303 (2008).

[31] S.-W. Lee and H. Jeong, Near-deterministic quantum teleportation and resource-efficient quantum computation using linear optics and hybrid qubits, Phys. Rev. A **87**, 022326 (2013).

[32] H. Jeong, A. Zavatta, M. Kang, S.-W. Lee, L. S. Costanzo, S. Grandi, T. C. Ralph, and M. Bellini, Generation of hybrid entanglement of light, Nature Photon **8**, 564 (2014).

[33] O. Morin, K. Huang, J. Liu, H. Le Jeannic, C. Fabre, and J. Laurat, Remote creation of hybrid entanglement between particle-like and wave-like optical qubits, Nature Photon **8**, 570 (2014).

[34] D. V. Sychev, A. E. Ulanov, E. S. Tiunov, A. A. Pushkina, A. Kuzhamuratov, V. Novikov, and A. I. Lvovsky, Entanglement and teleportation between polarization and wave-like encodings of an optical qubit, Nat. Commun. **9**, 3672 (2018).

[35] A. Cavaillés, H. Le Jeannic, J. Raskop, G. Guccione, D. Markham, E. Diamanti, M. D. Shaw, V. B. Verma, S. W. Nam, and J. Laurat, Demonstration of Einstein-Podolsky-Rosen Steering Using Hybrid Continuous- and Discrete-Variable Entanglement of Light, Phys. Rev. Lett. **121**, 170403 (2018).

[36] P. van Loock, Optical hybrid approaches to quantum information, Laser Photonics Rev. **5**, 167 (2011).

[37] U. L. Andersen, J. S. Neergaard-Nielsen, P. van Loock, and A. Furusawa, Hybrid discrete- and continuous-variable quantum information, Nat. Phys. **11**, 713 (2015).

[38] H. Wiseman and G. Milburn, *Quantum Measurement and Control* (Cambridge University Press, Cambridge, 2010).

[39] T. Chanelière, D. N. Matsukevich, S. D. Jenkins, T. A. B. Kennedy, M. S. Chapman, and A. Kuzmich, Quantum Telecommunication Based on Atomic Cascade Transitions, Phys. Rev. Lett. **96**, 093604 (2006).

[40] B. Srivathsan, G. K. Gulati, B. Chng, G. Maslennikov, D. Matsukevich, and C. Kurtsiefer, Narrow Band Source of Transform-Limited Photon Pairs via Four-Wave Mixing in a Cold Atomic Ensemble, Phys. Rev. Lett. **111**, 123602 (2013).

[41] G. K. Gulati, B. Srivathsan, B. Chng, A. Cerè, and C. Kurtsiefer, Polarization entanglement and quantum beats of photon pairs from four-wave mixing in a cold ^{87}Rb ensemble, New J. Phys. **17**, 093034 (2015).

[42] K. Wang, S. Shi, W. Zhang, Y. Ye, Y. Yu, M. Dong, Y. Zhai, D. Ding, and B. Shi, Experimental demonstration of two-color Einstein-Podolsky-Rosen entanglement in a hot vapor cell, OSA Continuum **2**, 2260 (2019).

[43] C. H. Bennett, G. Brassard, C. Crépeau, R. Jozsa, A. Peres, and W. K. Wootters, Teleporting an Unknown Quantum State Via Dual Classical and Einstein-Podolsky-Rosen Channels, Phys. Rev. Lett. **70**, 1895 (1993).

[44] J.-W. Pan, Z.-B. Chen, C.-Y. Lu, H. Weinfurter, A. Zeilinger, and M. Żukowski, Multiphoton entanglement and interferometry, Rev. Mod. Phys. **84**, 777 (2012).

[45] A. I. Lvovsky, Squeezed light, in *Photonics Volume 1: Fundamentals of Photonics and Physics*, edited by D. Andrews (Wiley, West Sussex, 2015), pp. 121–164.

[46] W. P. Bowen, N. Treps, B. C. Buchler, R. Schnabel, T. C. Ralph, H.-A. Bachor, T. Symul, and P. K. Lam, Experimental investigation of continuous-variable quantum teleportation, Phys. Rev. A **67**, 032302 (2003).

[47] X. Jia, X. Su, Q. Pan, J. Gao, C. Xie, and K. Peng, Experimental Demonstration of Unconditional Entanglement Swapping for Continuous Variables, Phys. Rev. Lett. **93**, 250503 (2004).

[48] N. Takei, H. Yonezawa, T. Aoki, and A. Furusawa, High-Fidelity Teleportation beyond the No-Cloning Limit and Entanglement Swapping for Continuous Variables, Phys. Rev. Lett. **94**, 220502 (2005).

[49] H. Yonezawa, S. L. Braunstein, and A. Furusawa, Experimental Demonstration of Quantum Teleportation of Broadband Squeezing, Phys. Rev. Lett. **99**, 110503 (2007).

[50] N. Lee, H. Benichi, Y. Takeno, S. Takeda, J. Webb, E. Huntington, and A. Furusawa, Teleportation of nonclassical wave packets of light, Science **332**, 330 (2011).

[51] D. F. Walls and G. J. Milburn, *Quantum Optics* (Springer-Verlag, Berlin, 2008).

[52] H. F. Hofmann, T. Ide, T. Kobayashi, and A. Furusawa, Information losses in continuous-variable quantum teleportation, Phys. Rev. A **64**, 040301(R) (2001).

[53] R. E. S. Polkinghorne and T. C. Ralph, Continuous Variable Entanglement Swapping, Phys. Rev. Lett. **83**, 2095 (1999).

[54] F. E. Becerra, R. T. Willis, S. L. Rolston, H. J. Carmichael, and L. A. Orozco, Nondegenerate four-wave mixing in rubidium vapor: Transient regime, Phys. Rev. A **82**, 043833 (2010).

[55] M. Dąbrowski, M. Parniak, and W. Wasilewski, Einstein-Podolsky-Rosen paradox in a hybrid bipartite system, Optica **4**, 272 (2017).

[56] N. Prajapati and I. Novikova, Polarization-based truncated SU(1, 1) interferometer based on four-wave mixing in Rb vapor, Opt. Lett. **44**, 5921 (2019).

[57] A. M. Akulshin, R. J. McLean, A. I. Sidorov, and P. Hannaford, Coherent and collimated blue light generated by four-wave mixing in Rb vapour, Opt. Express **17**, 22861 (2009).

[58] M. B. Kienlen, N. T. Holte, H. A. Dassonville, A. M. C. Dawes, K. D. Iversen, R. M. McLaughlin, and S. K. Mayer, Collimated blue light generation in rubidium vapor, Am. J. Phys. **81**, 442 (2013).

[59] S. H. Lie and H. Jeong, Limitations of teleporting a qubit via a two-mode squeezed state, Photon. Res. **7**, A7 (2019).